22nd Australasian Fluid Mechanics Conference AFMC2020
Brisbane, Australia, 6-10 December 2020
DOI: 10.14264/uql.2020.xxyy

Stereo PIV study of multirotor UAV downwash and spray dispersion

I.Chyrva[1], N. Kabaliuk[1], C. Dunker[2], T. Strand[3], P. Geoghegan[4], M. Jermy[1]

[1]Department of Mechanical Engineering

University of Canterbury, Christchurch, New Zealand

[2]Rocket Lab USA

Auckland, New Zealand

[3]Scion

Christchurch, New Zealand

[4] Aston University, Birmingham, UK

Abstract

Multirotor unpiloted aerial vehicles are increasingly used for agricultural spraying. Spray dispersion is complicated by the interaction of adjacent rotor flows. Stereo PIV was used to map the flow field of a multicopter in a wind tunnel, to determine the effect of adjacent rotors and horizontal velocity. Spray droplet trajectories were modelled as they passed through the measured air velocity field. Comparisons were made to measured spray deposition patterns. Nozzle position plays an important role in spray dispersion and loss to wind drift. Placing the nozzle in the fastest part of the downwash is recommended. Zones of upward air motion at the tips of front and side rotors can exacerbate wind drift, and cause spray to impinge on the multicopter body.

Keywords

Multirotor; UAV; RPAS; spray; agriculture; rotor aerodynamics

Introduction and motivation

Unmanned aerial vehicles (UAVs) are increasingly used in the agricultural sector. They are precise tools for small tasks where larger piloted aircraft would significantly increase the cost or hazard of an operation. UAVs are increasingly used in crop disease monitoring and delivery of agricultural spray. The advantage is marked for small areas of crop and on steep terrain.

For predicting spray dispersion from piloted aircraft, the software package AGDISP [1] is widely accepted by regulators. It includes a model for predicting the airflow around a helicopter or fixed wing craft, but cannot model the airflow around multicopters due to the interaction between rotors, and the lower flight speed [2].

Richardson et al. [3] used a modified DJI Agras MG-1 multicopter and measured the deposited spray pattern. The position of nozzles relative to the rotors was found to have a significant effect on the spray uniformity. Guo et al. [4] found that the spray pattern is strongly correlated with the vortex structure created by the rotors. Wang et al. [5] used a centrifugal atomiser nozzle and concluded that spray drift was difficult to predict at wind speeds above 3.86 m/s. These studies raise the questions: what is the influence of the downwash on the spray pattern, and what is the optimum position of the nozzles on a multicopter for spraying?

The downwash can affect the spray distribution on the ground and, possibly, enhance or reduce drift of the spray to off-target areas. The present work quantifies the effect of downwash on spray distribution for a particular rotor system.

Figure 1 shows the results of preliminary light sheet imaging used to visualize the dispersion of spray from a nozzle placed under a pair of counter-rotating UAV rotors (average of 100 images). The rotors were APC 1047 (10" diameter, 4.7" pitch, Landing Products Inc., Woodland, CA, USA https://www.apcprop.com/files/PER3_10x47.dat accessed 09.07.2020), with 254 mm diameter, at 5400 RPM. The rotor shafts were 280 mm apart, i.e. tip arcs were separated by 26 mm. The nozzle was placed at 60% of the rotor radius from the axis (0.6R), which places it in the highest downwash velocity. The nozzle was a Teejet TXA 800050VK spraying water at 3 bar (ASABE 'Very Fine' category). A horizontal air velocity of 2 m/s (from right to left) was applied with the UC open jet wind tunnel. Figure 1 shows light sheet images of the spray. In the left image, the rotors are switched off, and in the right image, they are switched on. The spray trajectory is influenced by the rotor downwash.

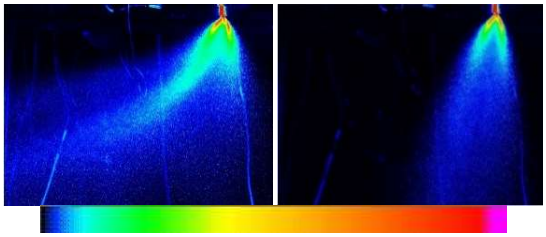

Figure 1 Light sheet images of a single Teejet TXA 800050VK nozzle at 3 bar in 2m/s cross flow: rotors off (left); rotors on (right). Purple colour is the saturation of image

Measuring spray deposition on the ground

Experimental procedure: hovering (zero lateral velocity)

Two DJI E7000 rotors (as used in UAVs with total mass >25 kg) were placed 3000 mm from the ground, with 86 mm separation between the tip arcs (Figure 2), rotating at 1740 rpm. The spray nozzle and pressure were the same as in Figure 1. Two nozzle positions were tested: (1) between rotors, 20mm below the rotor plane (Figure 2, top right) and (2) 0.6R from the centre of the rotor (Figure 2). In both cases, the nozzle tip was 60mm below the rotor plane.

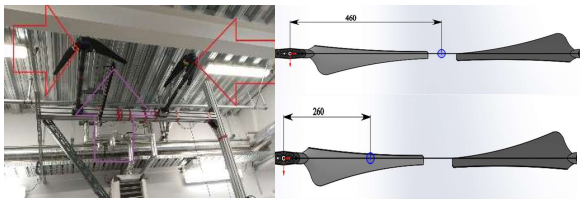

Figure 2 Experimental setup for the testing of spray deposition pattern. DJI E7000 system. Two rotors (red arrows). Labelled items are: rotors (red arrows), nozzle (purple arrow).

Styrofoam sheets were laid on the ground and water with blue dye was sprayed for 60 seconds. An image of the Styrofoam was processed using ImageJ. The image was binarized and divided into interrogation windows with 16x16 pixels size. In each window, the number of white pixels was calculated. The result is shown in Figure 3 where the colour contours represent the coverage of the Styrofoam i.e 100% (red) is fully covered by a liquid, 0% (white) has no liquid detected. The arrow marks a position vertically underneath the nozzle. The linear artefact is due to the join between two sheets of Styrofoam. Here, a 2.4 mm step in surface level affects the near-surface flow.

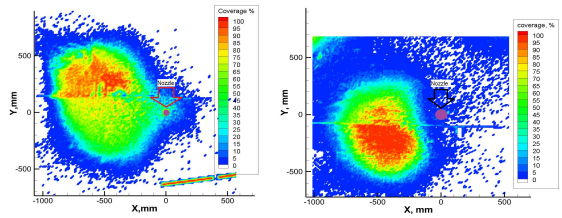

Figure 3 Spray deposition pattern on the ground (zero horizontal velocity): nozzle between rotors (left), nozzle placed underneath the fastest downwash (right).

In both cases, the centre of mass of the deposited spray footprint is shifted relative to the nozzle. Spray released from a nozzle in the region of fastest downwash (0.6R) is more concentrated i.e. has a smaller footprint, compared to spray released between the rotor discs. The area with 50% or greater coverage was 0.67 m^2 if the nozzle was placed under the greatest downwash, and 0.90 m^2 if the nozzle is placed between rotor disks. With the nozzle between the rotors, some water was found on the walls (1.5 m away), suggesting that the rotors are in ground effect with the downwash spreading radially where it meets the floor. The lateral motion of the spray is less severe with the nozzle under the rotor.

Computation of velocity field with lateral velocity:

To isolate rotor-rotor interaction, the multicopter was represented by a pair of rotors, spinning in opposite directions, sharing the same rotor plane. The University of Canterbury open-jet wind tunnel was used to provide the lateral velocity that an aircraft experiences when flying horizontally (Figure 4). The tunnel jet is 1500 x 1500 mm in cross-section. The rotors were arranged either: a) one downstream of the other ("arranged streamwise") or b) side by side ("arranged spanwise"). The horizontal distance between the rotor axes was varied. The rotors were APC 1047 units. Different rotational speeds were tested (2550 RPM to 7500 RPM) but only 5400 RPM data is presented here. This speed is typical for a hovering multicopter. The blades used were smaller than those used for commercial agricultural spraying, but they fit into the wind tunnel jet, and previous work with 840 mm diameter DJI (DJI, Shenzhen, China) rotors showed they are aerodynamically similar to an acceptable degree (i.e. thrust coefficient (C_T=0.14), power coefficient (C_P=0.063) and tip Mach number (Ma=0.21) are within 20% of the DJI rotor values), that the downwash structure is has a similar structure, and both rotor types have similar peak downwash velocity (11.2 m/s at 0.6R for APC 1047 and 10.6 m/s for DJI at 0.6 R).

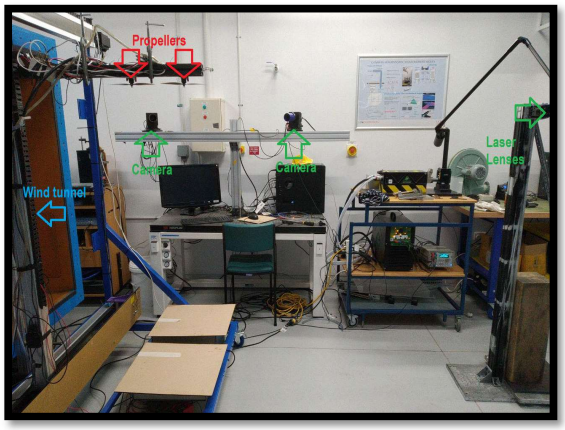

Figure 4 Wind tunnel setup. Labelled items are: rotors (red arrows, in the streamwise configuration), SPIV cameras and light sheet optics (green arrows) and wind tunnel (blue arrow, pointing opposite to the direction of flow).

Flight speeds (wind tunnel jet speeds) tested were 2m/s, 6m/s, 10m/s and 14m/s. For efficient operation and control, multicopter spraying usually uses a flight speed of around 6m/s.

SPIV (Stereo Particle Image Velocimetry) used a 15Hz dual cavity 150mJ frequency-doubled Nd:YAG EverGreen (70-200 mJ @ 532 nm, Lumibird, Köln, Germany) laser and two cameras (TSI 4MPa, Model l630091 Power View™ 4MP– HS Camera, TSI, Shoreview, MN, USA) viewing at +25°, -25° from a normal to the light sheet (Figure 4). The 2mm thick light sheet was generated with a Dantec guide arm and light sheet optics. Seed particles of 10% glycerin 90% water (v/v) were generated with a set of Laskin nozzles (four 0.5mm diameter holes in each copper pipe, fed with air at 6 bar, Figure 5) [6]. Seven to ten particles per interrogation window were seen. The size of the particles is estimated to be 1-10 microns. The maximum velocity magnitude observed in experiment was 18 m/s (blade tip vortex). Assuming that particle size was 10 microns and the maximum Stokes number should not exceed 1, the minimum diameter of vortex that could be successfully captured by PIV is 7 mm.

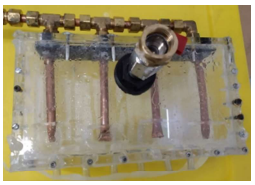

Figure 5 Laskin seeder

Images were acquired when the rotors were parallel to each other (tips at farthest approach). Image acquisition was triggered by optical interrupters on each of the rotor shafts and AND gate. 50 images were obtained for each plane.

Data were processed with the TSI Insight 4G package using background subtraction, ensemble averaging with Nyquist grid processor, and interrogation window refinement from 64x64 to 32x32 pixels. Global and local vector validation algorithms (validating against the local median value of all vectors in the neighbourhood) were used to validate the vector

field obtained while experimenting. The field of view was 428x296mm with a pixel size of 167 microns. Residual error (discrepancy between left and right cameras) and standard uncertainty (using the peak to noise ratio) for planar vector files were evaluated using Insight 4G [7]. The uncertainty is dependant on lateral velocity. The ratio of standard uncertainty to mean was < 8% in the downwash jet, but exceeded 50% outside the jet due to the small mean velocities.

The rotors were mounted on a ballscrew traverse and were traversed through the light sheet in a horizontal direction normal to the wind tunnel flow in 5 mm increments (some data was acquired at 10 mm increments). For each experiment, 62 to 75 planes were acquired. 3D fields were reconstructed in Tecplot Focus 2013 R1 (Tecplot, Bellevue, WA, USA) using kriging to interpolate between planes[8].

A vertical plane through SPIV data (Figure 6) shows that the leeward downwash is shadowed by the windward downwash, and the leeward downwash tilts to the vertical by 20-25° less than the windward downwash. This was observed for the whole range of lateral velocities from 2m/s to 14m/s. The purple/red region represents the zone of tip vortex; yellow/green region is the region of greatest velocity. The blue regions on the top of the figure are the zone between two rotors and the zone under the hub of the rotor (Figure 6).

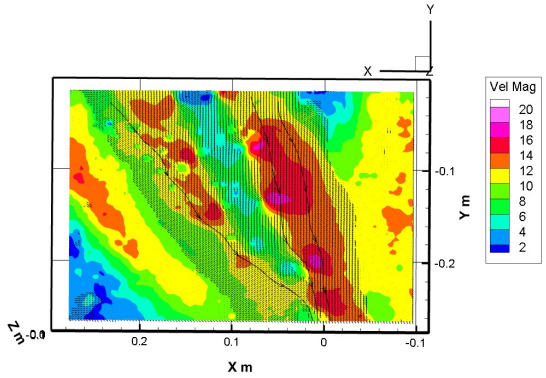

Figure 6 Velocity magnitude and streamlines on vertical planes through the axes of the rotors showing the tilt of the downwash of the front and rear rotors. Lateral velocity 6 m/s

A horizontal plane through the PIV data (Figure 7) shows that the windward rotor downwash forms into a horseshoe shape around the second rotor. The lee rotor downwash shape remains circular.

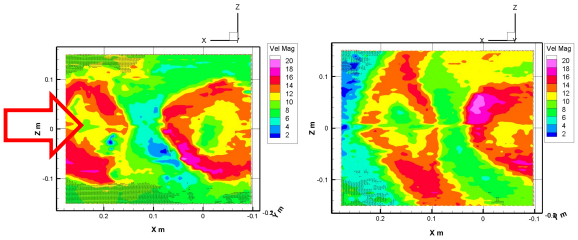

Figure 7 Velocity magnitude on horizontal planes below the rotor at flight speed 6m/s: left) 10 mm below the rotor plane; right) 200mm below the rotor plane. Lateral velocity 6 m/s. Red arrow indicates the lateral velocity direction (-x)

There are regions of upward-directed air formed at the tip of the rotor (Figure 8). This was observed only in the presence of the lateral velocity. Spray particles trapped in this region, if sufficiently low diameter, will likely travel upwards, decreasing the efficiency of spray application, and possibly entering the motors or electronics. This upward velocity region is present with both positions of the rotors shown in Figure 8.

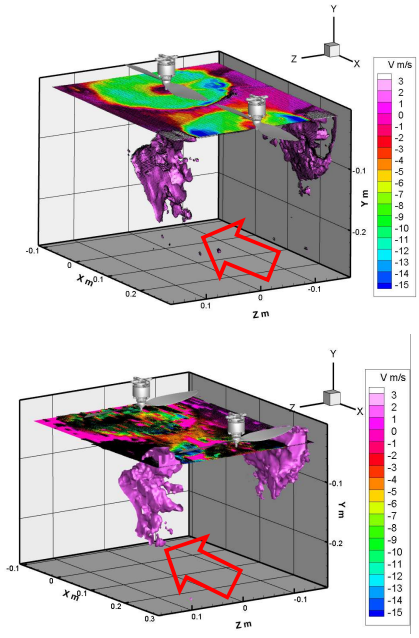

Figure 8 Iso-surface of vertically upward air velocity V_y=+2m/s at a flight speed of 6 m/s when rotors are parallel to the lateral velocity vector (top) and flight speed 6 m/s when rotors are perpendicular to the lateral velocity vector (bottom). Red arrow indicates the lateral velocity direction (-x)

The same upward-velocity region was observed for rotors arranged spanwise. If the region between the rotors is exposed to the lateral velocity (not shielded by downwash) an additional region of upward air motion is present there. In the presence of lateral velocity the strength of upward velocity region depends principally on the lateral velocity (Figure 9).

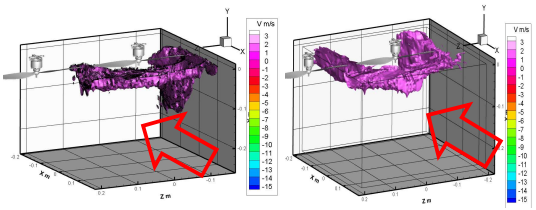

Figure 9 Iso-surface of vertically upward air velocity V_y=+2m/s; flight speed: 6m/s (left); 10m/s (right). Red arrow indicates the lateral velocity direction (-x).

Modelling of spray in lateral velocity downwash

Comparison of spray trajectories in the downwash and experimental analysis of spray outlet velocities

Virtual spray droplets were tracked from an assumed nozzle position, through the airflow field obtained with SPIV, with a Lagrangian method using the algorithm implemented in Tecplot Focus 2016 R1, including aerodynamic drag and gravitational forces. The drag coefficient is calculated from a correlation found in [8]. From early work with a droplet deformation model [5], deformation is not expected to affect the trajectories.

To mimic common agricultural nozzles, droplets of diameter 100 microns (i.e. the centre of the Very Fine (VF) (VMD range 60-145 micron) ASABE S-572.1 range [9]) and 300 microns (Medium (M) (VMD range 226-325 micron)) were tracked. Additionally, 600 micron diameter droplets (Extremely Coarse (EC) were tracked, but were influenced very little by the downwash. The initial speed of the droplets, on leaving the nozzle, was 12 m/s (measured by PIV around 5 mm from the nozzle exit with Teejet Conejet TXA800050VK nozzle, water pressure 3 bar). Droplets were released from several points within a spray cone of included angle 80°.

Different nozzle positions and droplet sizes were tested. Placing the nozzle in the region of fastest downwash is recommended because it limits drift from wind and delivers spray (especially in the VF range) directly to the sprayed surface. Figure 10 shows that some of the droplets in VF size range are carried away by the lateral velocity because they fall away from the zone of greatest downwash. Most of the spray is carried towards the ground by the downwash. 300 micron droplets were less influenced by the downwash and front spray trajectories show that this size requires around 0.2-0.3 m of travel from the nozzle orifice to change its trajectory and follow the downwash.

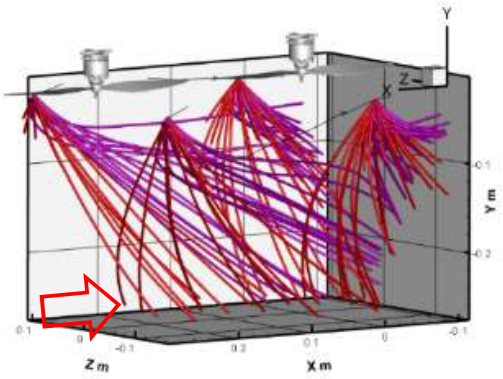

Figure 10 spray trajectories modelled within the PIV data. Nozzles placed under the strongest downwash, with 6m/s lateral velocity. Purple lines trajectories of 100 micron droplets, red lines 300 micron droplets. Red arrow indicates the lateral velocity direction (-x)

It is recommended that nozzles are not placed near the zones of upward velocity. Figure 11 shows the trajectories of droplets from a nozzle in one of these regions. The black spray trajectories represent the VF spray from the nozzle placed between rotors. The white zones in the colour contour slice are the strongest upward velocity regions.

Conclusions

For a hovering craft, the footprint of the spray was smaller if the nozzle was located between the rotors. However, for non-zero flight velocities, it is highly recommended to avoid placing the nozzle anywhere where the tip of the rotor passes, especially in the zone between rotors, because some spray will be drawn upwards, decreasing the efficiency of spraying and potentially entering the craft's electrical components.

By choosing the correct nozzle placement, smaller spray particles can be delivered to the target without drift caused by lateral velocity (wind, forward or side motion of the craft). The recommended position is the zone of strongest downwash. This location depends on the type of rotor but generally is between 0.5-0.7 times the rotor radius.

Acknowledgements

We are very grateful to SCION for funding this study.

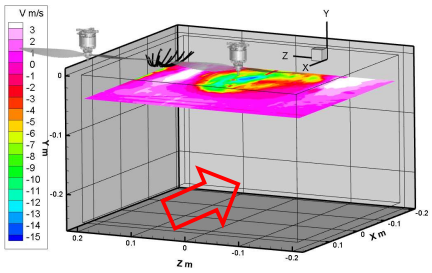

Figure 11 Spray trajectories modelled inside of PIV data. Nozzle placed in the region of upward velocity between rotors. Lateral velocity 10 m/s. Red arrow indicates the lateral velocity direction (-x)

References

1. Teske, M. E., Bird, S. L., Esterly, D. M., Curbishley, T. B., Ray, S. L., & Perry, S. G. (2002). AgDrift®: A model for estimating near-field spray drift from aerial applications. *Environmental Toxicology and Chemistry*, *21*(3), 659–671. https://doi.org/10.1002/etc.5620210327

2. Teske, M. E., Wachspress, D. A., Thistle, H. W., & Service, F. (2018). Prediction of aerial spray release from UAV's, *61*(3), 909–918. https://doi.org/10.13031/2013.31005.

3. Richardson, B., Rolando, C. A., Somchit, C., Dunker, C., Strand, M., & Kimberley, M. O. (2019). Swath pattern analysis from a multi-rotor unmanned aerial vehicle configured for pesticide application. *SCI*, (October). https://doi.org/10.1002/ps.5638

4. Guo, S., Li, J., Yao, W., Zhan, Y., Li, Y., & Shi, Y. (2019). Distribution characteristics on droplet deposition of wind field vortex formed by multi-rotor UAV. *PLoS ONE*, *14*(7), 1–16. https://doi.org/10.1371/journal.pone.0220024

5. Wang, G., Han, Y., Li, X., Andaloro, J., Chen, P., Hoffmann, W. C., … Lan, Y. (2020). Field evaluation of spray drift and environmental impact using an agricultural unmanned aerial vehicle (UAV) sprayer. *Science of the Total Environment*, *737*, 139793. https://doi.org/10.1016/j.scitotenv.2020.139793

6. Raffel, M., Willert, C. E., Wereley, S. T., & Kompenhans, J. (2007). *Particle image velocimetry* (Second edi.). Berlin: Springer. https://doi.org/10.1007/978-3-540-72308-0

7. *Insight 4G™ global image, acquisition, analysis, & display software*. (2015) (P/N 600511.). Shoreview, MI: TSI Incorporated. https://doi.org/https://www.tsi.com/product-components/insight-4g-version-11-2-global-imaging,-acquisition,-analysis-and-display-software/

8. *Tecplot 2013 User ' s Manual*. (2013) (Release 1/.). Bellevue, WA: Tecplot, inc. https://doi.org/https://www.tecplot.com/documentation/

9. *ASABE-Standards, S572.1, SprayNozzle Classification by Droplet Spectra. American Society of Agricultural and Biological Engineering,*. (2009). St. Joseph, MI (2009). https://doi.org/https://www.asabe.org/